# Dynamics of a mobile impurity in a two-leg bosonic ladder

Naushad Ahmad Kamar [1], Adrian Kantian,[2] and Thierry Giamarchi[1]

[1]*DQMP, University of Geneva, 24 Quai Ernest-Ansermet, 1211 Geneva, Switzerland*
[2]*Department of Physics and Astronomy, Uppsala University, Box 516, S-751 20 Uppsala, Sweden*

We analyze the behavior of a mobile quantum impurity, restricted to a one-dimensional motion, in a bath formed by a two-leg bosonic ladder through a combination of field theory [Tomonaga-Luttinger liquid (TLL)] and numerical (density-matrix renormalization group) techniques. We compute the Green's function of the impurity as a function of time at different momenta. We find a power-law decay at zero momentum, which signals the breakdown of a quasiparticle description of the impurity motion. We compute the exponent both for the limits of weak and strong impurity-bath interactions. At small impurity-bath interaction, the impurity experiences the ladder as a single channel one-dimensional bath, but with an effective coupling reduced by a factor of $\sqrt{2}$. We compare the numerical results for the exponent at zero momentum with a semianalytical expression, initially established for the chain, and find excellent agreement without adjustable parameters. We find an increase of the exponent with increasing transverse tunneling in the bath. At small tunneling, the exponent is compatible with the TLL prediction, while larger tunneling shows strong deviations. Finally, we show that, as a function of the momentum of the impurity, two different regimes of decay of the Green's function exist, similar to the single chain case. The power-law regime occurs for small momentum, while at large momentum the Green's function shows a faster decay, corresponding to the one expected in a polaronic regime. In this last regime, we compute the lifetime of the polaron numerically. We compute the critical momentum marking the transition between these two regimes. We compare with analytical predictions based on the structure factor of the bath and find good agreement with the numerical results. Finally, we discuss the consequences of our results for cold atomic experiments.

## I. INTRODUCTION

How a quantum environment can affect the properties of a quantum particle is one of the central problems for quantum many-body systems. In a solid, where the bath is formed by phonon excitations, this is at the heart of the polaron problem [1,2]. For interacting particles, the dressing of one particle by the excitations of the density induced by the interactions leads to the Fermi liquid description of an interacting fermion gas [3,4]. In addition to these types of effects, it was realized by Caldeira and Leggett that the environment can deeply change the properties of a quantum degree of freedom in a way that goes beyond the formation of a polaron with its attendant redefinition of some physical parameters of the particle, such as the mass [5,6]. Cold atomic systems provide a remarkable playground to investigate these issues, and the polaronic questions were thus intensively studied in this context (see. e.g., Ref. [7] and references therein).

One potentially important ingredient is the dimensionality of the system. It has been shown [8] that for a one-dimensional bath the influence on the propagation of the particle can be drastic. The particle motion may become subdiffusive with no remnant of quasiparticle behavior. The source for the onset of this dynamical universality class in the one-dimensional systems is a phenomenon akin to the Anderson orthogonality catastrophe. Following this result, the phenomenon was the subject of extensive studies [9–14]. Combining numerical and analytical results [15] showed that depending on the momentum of the particle a change in regime, from subdiffusive to polaronic, could occur. Extensions of these results to fermionic systems [16,17], driven particles [18,19], spinor impurities [20], or particles coupled to several one-dimensional systems [21] have since been performed.

On the experimental front, cold atomic systems have brought an unprecedented level of control to study these issues for low-dimensional systems [22–25], since they allow for excellent control of the interaction between the impurity and the bath, as well as direct measurements of correlation functions.

How the breakdown of the quasiparticle picture and the emergence of subdiffusive dynamics would be affected when either the dimensionality of impurity motion or the dimensionality of the bath increases is an open and interesting question. Indeed, in other effects in which orthogonality manifests, such as the x-ray edge problem [26], it is well known that in dimensions greater than one the onset of the orthogonality catastrophe is suppressed as soon as the impurity experiences recoil (i.e., impurity is mobile). This immediately gives rise to the question as to how one actually crosses over from the singular physics of a one-dimensional system to the more conventional polaronic dynamics [7] that one could naively expect for two- or three-dimensional baths.

In this paper, we address this issue by looking at an impurity propagating in a ladder. We still confine the impurity to move one dimensionally, but the bath has now a transverse extension. This allows separating the effects of the dimensionality of the bath from the ones of the impurity motion. The

case of the impurity with transverse motion will be examined elsewhere. We mostly focus on the case of a two-leg ladder but will also discuss some of the consequences of increasing the number of legs, to bridge the gap towards a two-dimensional bath. We analyze this problem using a combination of analytical and numerical techniques in a spirit similar to the one used for the single chain [15], and compare the results of the ladder bath to the known results for the single chain.

The plan of the paper is as follows. Section II presents the model, the various observable studied, and the bosonization representation that will be at the heart of the analytical analysis. Section III presents the two main analytical approaches that are used, namely a field theory representation based on the bosonization technique and a linked cluster expansion representation. Section IV presents the numerical density matrix renormalization group (DMRG) [27,28] analysis of this problem, and the results for the Green's function of the impurity. Section V discusses these results both in connection with the single chain results and in view of the possible extensions. Finally, Sec. VI concludes the paper and presents some perspectives in connection with experiments. Technical details can be found in the Appendixes.

## II. MOBILE IMPURITY IN A TWO-LEG BOSONIC LADDER

### A. Model

We consider a mobile impurity moving in a two-leg bosonic ladder. In this study, we restrict the motion of the impurity to be strictly one dimensional; other cases will be considered elsewhere [29]. This model is thus the simplest basic model for exploring the dynamics of a one-dimensional impurity in an environment that is no longer purely 1D itself.

The model we consider is depicted in Fig. 1. The full Hamiltonian is given by

$$H = H_K + H_{\text{lad}} + U \sum_j \rho_{1,j} \rho_{\text{imp},j}. \qquad (1)$$

$U$ is the interaction strength between the particles in the ladder and the impurity.
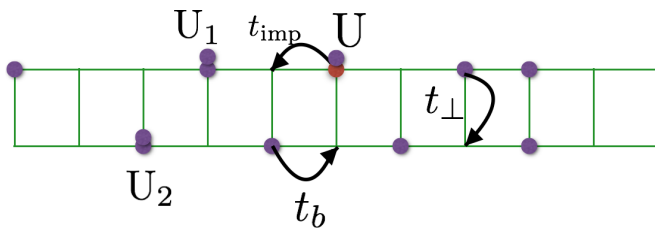


FIG. 1. Impurity in a two-leg bosonic ladder: solid magenta circles represent the bath particles and the red circle represents the impurity. The bath particles move along the legs (between the legs) with hopping $t_b$ ($t_\perp$) and have a contact interaction $U_1$ ($U_2$) between themselves (see text). The impurity motion is restricted to the upper leg and its amplitude is $t_{\text{imp}}$ (see text). The impurity and the bath particles interact by a contact interaction $U$. We have taken the $t_b = 1$, and all the interaction parameters are defined in the unit of $t_b$. $U_1 = U_1/t_b$, $U_2 = U_2/t_b$, $t_{\text{imp}} = t_{\text{imp}}/t_b$, and $t_\perp = t_\perp/t_b$ are dimensionless parameters.

The impurity kinetic energy is given by the tight-binding Hamiltonian

$$H_K = -t_{\text{imp}} \sum_j (d_{j+1}^\dagger d_j + \text{H.c.}), \qquad (2)$$

where $d_j$ ($d_j^\dagger$) are the destruction (creation) operators of the impurity on site $j$. The density of the impurity on site $j$ is

$$\rho_{\text{imp},j} = d_j^\dagger d_j. \qquad (3)$$

The ladder Hamiltonian $H_{\text{lad}}$ is given by

$$H_{\text{lad}} = H_1^0 + H_2^0 - t_\perp \sum_j (b_{1,j}^\dagger b_{2,j} + \text{H.c.}), \qquad (4)$$

where $b_{a,j}$ ($b_{a,j}^\dagger$) are the destruction (creation) operators of a boson of the bath on chain $a$ and site $j$. The $b$ operators obey the standard bosonic commutation relation rules. The single chain Hamiltonian is the Bose-Hubbard one:

$$H_i^0 = -t_b \sum_j (b_{j+1}^\dagger b_j + \text{H.c.}) + \frac{U_i}{2} \sum_j \rho_{i,j}(\rho_{i,j} - 1)$$
$$- \mu_i \sum_j \rho_{i,j}. \qquad (5)$$

In the following, we use the tunneling rate $t_b$ of the bath bosons as the unit of energy.

The form (1) is convenient for the numerical study. To make an easy connection with the field theory analysis, we can also consider the same problem in a continuum. In this case, the Hamiltonian becomes

$$H = \frac{P^2}{2M} + H_{\text{lad}} + U \int dx \, \rho_1(x) \rho_{\text{imp}}(x), \qquad (6)$$

where $P$ and $M$ are respectively the momentum and mass of the impurity. The density of the impurity is

$$\rho_{\text{imp}}(x) = \delta(x - X), \qquad (7)$$

where $X$ is the position of the impurity, canonically conjugate to $P$ so that $[X, P] = i\hbar$. We set from now on $\hbar = 1$.

In the continuum, the ladder Hamiltonian (4) becomes

$$H_{\text{lad}} = H_1^0 + H_2^0 - t_\perp \int dx [\psi_1^\dagger(x) \psi_2(x) + \text{H.c.}] \qquad (8)$$

and the single chain Hamiltonian is

$$H_i^0 = \frac{1}{2m} \int dx |\nabla \psi_i(x)|^2 + \frac{U_i}{2} \int dx \, \rho_i(x)^2$$
$$- \mu_i \int dx \, \rho_i(x). \qquad (9)$$

$m$ is the mass of the bosons, $\mu_i$ is the chemical potential, and $U_i$ is the intrachain interaction of leg $i = 1, 2$. $\psi(x)^\dagger$ [$\psi(x)$] is the creation (annihilation) operator at position $x$.

### B. Observables

To characterize the dynamics of impurity in the ladder bath, we mostly focus on the Green's function of the impurity. We study it both analytically and numerically via DMRG, each time considering the zero temperature case. The Green's

function of the impurity is defined as

$$G(p,t) = \langle \hat{d}_p(t)\hat{d}_p^\dagger(t=0)\rangle, \tag{10}$$

where $\langle \cdots \rangle$ denotes the average in the ground state of the bath, and with zero impurities present. $O(t)$ denotes the usual Heisenberg time evolution of the operator

$$O(t) = e^{iHt}O\,e^{-iHt} \tag{11}$$

and the operator $\hat{d}_p$ is the operator destroying an impurity with momentum $p$ given by

$$\hat{d}_p = \sum_j e^{ipr_j}d_j, \tag{12}$$

with $r_j = aj$ on the lattice and the corresponding integral

$$\hat{d}_p = \int dx\, e^{ipx}d(x) \tag{13}$$

in the continuum.

### C. Bosonization representation

To deal with the Hamiltonian defined in the previous section, it is convenient to focus on the relevant low-energy, long-wavelength properties using the so-called bosonization representation. This representation is well documented in the literature by now, and we recall here only the salient points to fix the notations.

The single-particle operators are represented in terms of two conjugate operators $\phi(x)$ and $\theta(x)$, capturing collective excitations of density and phase, respectively, via the formulas [26]

$$\rho_\alpha(x) = \rho_{0,\alpha} - \frac{\nabla\phi_\alpha(x)}{\pi} + \rho_0\sum_{p\neq 0}e^{2ip[\pi\rho_{0,\alpha}x-\phi_\alpha(x)]}, \tag{14}$$

where $\rho_{0,\alpha}$ is the average density on the chain $\alpha = 1,2$. The creation operator of a particle in the bath in terms of $\theta$ and $\phi$ is given to lowest order by

$$\psi_\alpha^\dagger(x) = \rho_{0,\alpha}^{1/2}e^{-i\theta_\alpha(x)}. \tag{15}$$

The conjugate field operators $\phi_{1,2}$ and $\theta_{1,2}$ obey

$$\left[\phi(x_1), \frac{\nabla\theta(x_2)}{\pi}\right] = i\delta(x_1-x_2). \tag{16}$$

Using the above representation, and assuming that the filling of the chains is not commensurate with the underlying lattice, allows rewriting the Hamiltonian of each chain as [26]

$$H_\alpha^0 = \frac{1}{2\pi}\int dx\left[u_\alpha K_\alpha(\partial_x\theta_\alpha)^2 + \frac{u_\alpha}{K_\alpha}(\partial_x\phi_\alpha)^2\right], \tag{17}$$

where $u_\alpha$ and $K_\alpha$ are the so-called Tomonaga-Luttinger liquid (TLL) parameters. Here, $u_\alpha$ is the velocity of density excitations (i.e., sound) in the chain, while $K_\alpha$ encodes the effect of interactions and controls the decay of the correlation functions. Their values can be directly related to the bare parameters of the given microscopic Hamiltonian [26,30]. For example, for the Lieb-Lininger model [31] of bosons in the continuum with contact interaction $K = \infty$ when the interaction is zero and $K = 1$ when the contact repulsion is

infinite. For the two-leg bosonic ladder the TLL parameters can be found in [32].

Using the bosonization framework, the low-energy approximation of interleg tunneling is

$$-2t_\perp\rho_0\int dx\,\cos[\theta_1(x)-\theta_2(x)]. \tag{18}$$

This makes it convenient to use the symmetric and antisymmetric combinations of the fields

$$\theta_{s,a} = \frac{\theta_1\pm\theta_2}{\sqrt{2}} \tag{19}$$

and analogous expressions for the fields $\phi_s(\phi_a)$. The new fields remain canonically conjugate and allow one to re-express the Hamiltonian of the bath as

$$H_{\text{lad}} = H_s + H_a, \tag{20}$$

with

$$H_s = \frac{1}{2\pi}\int dx\left[u_s K_s(\partial_x\theta_s)^2 + \frac{u_s}{K_s}(\partial_x\phi_s)^2\right],$$

$$H_a = \frac{1}{2\pi}\int dx\left[u_a K_a(\partial_x\theta_a)^2 + \frac{u_a}{K_a}(\partial_x\phi_a)^2\right]$$
$$\quad - 2\rho_0 t_\perp\int dx\,\cos[\sqrt{2}\theta_a(x)]. \tag{21}$$

Because of the presence of the cosine term the antisymmetric part of the Hamiltonian (the so-called sine-Gordon Hamiltonian) will be massive when $K_a > 1/4$. As a result the field $\theta_a$ is locked to the minima of the cosine indicating the phase coherence across the two legs of the ladder. The phase being locked, the density fluctuation in the antisymmetric sector has fast decaying correlations instead of the usual power law of the TLL. The symmetric sector remains massless with power-law correlations. A numerical calculation of the TLL parameters for the massless phase can be found in [32].

### III. ANALYTICAL SOLUTIONS

Let us now investigate the full Hamiltonian (6) [or (1)] to be able to compute the Green's function of the impurity (10).

Using (14) the interaction term $H_{\text{coup}}$ with the impurity is expressed, as a function of the bosonized variables as

$$H_{\text{coup}} = \frac{-U}{\sqrt{2}\pi}\int dx[\nabla\phi_a(x) + \nabla\phi_s(x)]\rho_{\text{imp}}(x)$$
$$\quad + 2U\rho_0\int dx\,\cos\{\sqrt{2}[\phi_a(x)+\phi_s(x)]$$
$$\quad - 2\pi\rho_0 x\}\,\rho_{\text{imp}}(x), \tag{22}$$

where we have retained only the lowest harmonics in the oscillating terms, with higher-order terms being *a priori* less relevant.

Since the antisymmetric sector is gapped, with a gap $\Delta_a$ due to the ordering in the field $\theta_a$, the correlation functions involving $\phi_a$ decrease exponentially at large distance or time interval. We thus *a priori* need to distinguish the cases for which $U \ll \Delta_a$, for which the interaction with the impurity is not able to create excitations in the antisymmetric sector, from the case $U \gg \Delta_a$. We examine these two cases in turn.

## A. $U \ll \Delta_a$

In this case, the coupling with the impurity cannot create excitations in the antisymmetric sector. The backscattering term containing $\cos\{\sqrt{2}[\phi_a(x) + \phi_s(x)]\}$ is thus irrelevant. This term can potentially generate a $\cos[2\sqrt{2}\phi_s(x)]$ term by operator product expansion (OPE) but such term would only become relevant for $K_s < 1$, which is outside the range of allowed TLL parameters for the bosonic problem we consider here.

Thus, as for the case of a single impurity [8], the forward scattering term gives the dominant contribution

$$\frac{-U}{\sqrt{2\pi}} \int dx \, \nabla \phi_s(x) \rho_{\mathrm{imp}}(x), \qquad (23)$$

in which we have kept only the part corresponding to the massless sector.

In this regime, the impurity behaves in the ladder system as it would be in a single chain with effective parameters $(u_s, K_s)$, but with a renormalized coupling

$$U_2 = \frac{U}{\sqrt{2}}. \qquad (24)$$

Note, however, that for a microscopic interaction $U_1 = U_2$ the TLL parameters $(u_s, K_s)$ will generally not be equal to the ones of a single chain with the corresponding interaction due to the presence of the irrelevant operators coming from the $t_\perp$ term. The Green's function of the impurity (10) can thus be readily computed by the same techniques used for the single chain case [8,15]. Using a linked cluster expansion (LCE), a resummed second-order perturbation series applicable at small bath-impurity interactions, as detailed in Appendix A, we find that, when $p < \frac{u_s}{2t_{\mathrm{imp}}}$, the difference of energies of the impurity $\epsilon_p - \epsilon_{p+q}$ intersects the bath dispersion $u_s|q|$ only at $q = 0$. As shown in Appendix A this leads to a power-law decay of the Green's function (10)

$$|G(p,t)| = e^{-\frac{K_s U^2}{4\pi^2 u_s^2}\left(1 + \frac{12 t_{\mathrm{imp}}^2 p^2}{u_s^2}\right)\ln(|t|)}. \qquad (25)$$

This case will be discussed in detail in Sec. IV B.

On the contrary, for $p > \frac{u_s}{2t_{\mathrm{imp}}}$, $\epsilon_p - \epsilon_{p+q}$ intersects the bath dispersion $u_s|q|$ at nonzero $q$'s. In that case the Green's function decays exponentially, as the impurity enters the so-called quasiparticle (QP) regime [15], where $\epsilon_p = -2t_{\mathrm{imp}}\cos(p)$. This case will be discussed in Sec. IV C.

The dynamical structure factor $S(k, \omega)$ of one leg of the ladder is given by

$$S(x, \omega) = \langle GS_b| \rho_1(x) \frac{1}{\omega + i\eta - H_{\mathrm{lad}}} \rho_1(0) |GS_b\rangle,$$

$$S(k, \omega) = \int dx \, S(x, \omega) \exp(-ikx), \qquad (26)$$

where $\eta \rightarrow 0^+$ and $\rho_1(x)$ is the density operator in leg 1 of the ladder at position $x$.

To go beyond the bosonized evaluation of the structure factor of the bath used in Appendix A, we also show in Fig. 2 the imaginary part of the dynamical structure factor defined in Fig. 2 computed using DMRG at $t_\perp = t_b = 1$, bond dimension $\chi = 600$, and zero temperature, together with $\delta\epsilon(q) = \epsilon_p - \epsilon_{p+q}$, for different $p$ values at $t_{\mathrm{imp}} = 1$. As
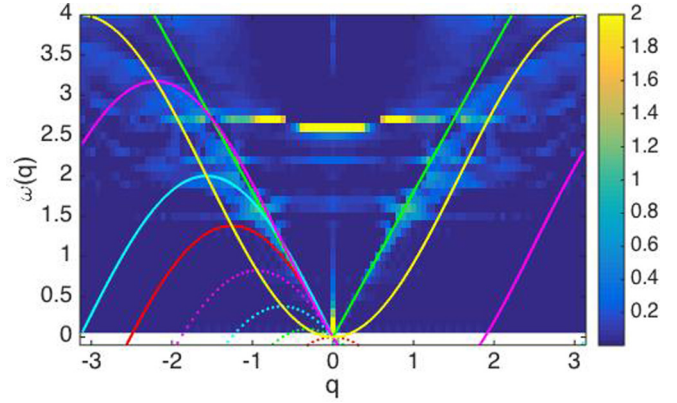


FIG. 2. Dynamical structure factor for leg 1 of the two-leg hardcore boson ladder at one-third filling (shaded area). Superimposed colored curves show the change in the impurities kinetic energy when emitting an excitation with momentum $q$ into the bath, $\delta\epsilon(q) = \epsilon_{\mathbf{p}} - \epsilon_{p+q}$, for different values of $p$. In ascending order by maximal value these are red ($p = 0$), green ($0.1\pi$), cyan ($0.2\pi$), magenta ($0.3\pi$), red ($0.4\pi$), cyan ($0.5\pi$), magenta ($0.7\pi$), and yellow ($\pi$). Dotted lines ($p = 0, 0.1\pi, 0.2\pi$) denote where $\delta\epsilon(q)$ intersects with areas of finite weight of the dynamical structure factor only at $q = 0$. Solid lines and dotted line at $p = 0.3\pi$ denote the higher $p$ values for which it intersects also at nonzero $q$'s. This change in regime causes the impurity to go from subdiffusive to quasiparticle behavior (see text).

would be expected, we find that for small $q$ the dispersion of bath is well fitted with the linear dispersion used in the TLL representation $u_s|q|$ (green line, $u_s = 1.8$). More importantly, the results in Fig. 2 deliver an expanded understanding of the transition between subdiffusive and quasiparticle dynamics. As discussed in more detail in Sec. IV C and Fig. 8, we find that, as also established via LCE previously, as long as $\delta\epsilon(q)$ intersects with the full structure factor-derived excitation spectrum only at $q = 0$, dynamics is subdiffusive ($p = 0, 0.1\pi, 0, 2\pi$). But the transition to QP dynamics actually sets in once $\delta\epsilon(q)$ intersects at $q \neq 0$ with the area where the ladder excitation spectrum has finite weight (i.e., for ($p = 0.3\pi, 0.4\pi, 0.5\pi, 0.7\pi, \pi$). This goes well beyond the transition criterion derived via LCE, as there we could only use the linearized low-energy component of the excitation spectrum.

## B. $U \gg \Delta_a$

We now consider the more complicated opposite case for which the interaction with the impurity, which couples to the field $\phi_1$, can potentially induce excitations across the antisymmetric gap for the field $\theta_1$. In order to deal with this case, we essentially follow the method introduced by Lamacraft for the case of the single chain [12].

We first make a transformation to a frame of reference which moves with the impurity, and this can be imposed by a unitary transformation $U_X = e^{i(P_1 + P_2)X}$, where $P_1$ and $P_2$ denote the momentum operators of first and second ladder leg, respectively, and $X$ denotes the impurity's position operator.

By using (6) and (7), the effective Hamiltonian in the new frame of reference is given by

$$
\begin{aligned}
H_{\text{eff}} &= U_X H U_X^\dagger \\
&= \frac{(P - P_1 - P_2)^2}{2M} + H_{\text{lad}} + U\rho_1(0),
\end{aligned}
\tag{27}
$$

where $\rho_1(0)$ is the density of leg 1 at $x = 0$. In the new effective Hamiltonian, the position operator $X$ has disappeared and $P$ is thus a conserved quantity. As $U \to \infty$, $U$ is replaced by an effective forward scattering potential $U_\phi$ (roughly the phase shift corresponding to the potential $U$) [12] and $\rho_1(x = 0) = -\int dx\, \delta(x) \frac{\nabla\phi_s(x) + \nabla\phi_a(x)}{\sqrt{2}\pi}$. The forward scattering can thus be absorbed in the quadratic terms $\frac{1}{2\pi} \frac{u}{K} \int dx (\nabla\phi(x))^2$ (for $s$ and $a$ fields) and creates a discontinuity in the fields $\phi_s$ and $\phi_a$ of the form [12]

$$
\begin{aligned}
\phi_s |_{0^+}^{0^-} &= \frac{K_s U_\phi}{\sqrt{2} u_s}, \\
\phi_a |_{0^+}^{0^-} &= \frac{K_a U_\phi}{\sqrt{2} u_a}.
\end{aligned}
\tag{28}
$$

The dominant term in the total current is given by

$$
P_1 + P_2 = \int dx\, \rho_0 \sqrt{2} \nabla\theta_s(x),
\tag{29}
$$

where in the above formula the origin must be excluded if the field has a discontinuity. For $P = 0$ the minimization of $H$ imposes that the field $\theta_s$ remains continuous at $x = 0$. These two sets of conditions for the fields $\phi$ and $\theta$ can be imposed on otherwise continuous fields by the unitary transformation

$$
U_{P=0} = \exp\left(i\theta_s(0)\frac{K_s U_\phi}{\sqrt{2}\pi u_s}\right) \exp\left(i\theta_a(0)\frac{K_a U_\phi}{\sqrt{2}\pi u_a}\right).
\tag{30}
$$

The impurity Green's function at zero momentum is thus given by

$$
\begin{aligned}
|G(0,t)| &= \langle U_{P=0,t}^\dagger U_{P=0,0} \rangle \\
&= \left\langle \exp\left(-i\theta_s(t)\frac{K_s U_\phi}{\sqrt{2}\pi u_s}\right) \exp\left(i\theta_s(0)\frac{K_s U_\phi}{\sqrt{2}\pi u_s}\right) \right\rangle \\
&= \left\langle \exp\left(-i\theta_a(t)\frac{K_a U_\phi}{\sqrt{2}\pi u_a}\right) \exp\left(i\theta_a(0)\frac{K_a U_\phi}{\sqrt{2}\pi u_a}\right) \right\rangle \\
&= |t|^{-K_s/4\left(\frac{U_\phi}{\pi u_s}\right)^2}.
\end{aligned}
\tag{31}
$$

To compute the above correlation function corresponding to field $\theta_a$ we have expanded $\cos(\sqrt{2}\theta_a)$ up to second order, and exploited that the correlation function of the antisymmetric mode saturates to a finite value for time greater than the inverse of gap in the antisymmetric sector. The symmetric mode decays as a power law with an exponent $\alpha = \frac{K_s}{4}\left(\frac{U_\phi}{\pi u_s}\right)^2$. For hard-core bosons in one dimension $\frac{U_\phi}{\pi u_s} = 1$, and thus the overall exponent in (31) is

$$
\alpha = K_s/4.
\tag{32}
$$

However, as will be discussed in more details in Sec. IV B 2, the case of the ladder is more complicated since $U_\phi$ can potentially depend on $t_\perp$.

## IV. NUMERICAL SOLUTION

### A. Method

To obtain the Green's function of the impurity for the ladder problem quantitatively, we compute a numerical solution of the lattice model defined in Sec. II A, by a method analogous to the one used for the single chain [15]. We use DMRG to compute the ground state of the bath and time-dependent DMRG (t-DMRG) to compute the Green's function of the impurity.

For t-DMRG, we use a supercell approach to map the three species of bosons $(A, B, C)$ onto a one-dimensional chain. Leg 1 and leg 2 of the ladder are represented by species $A$ and $B$, respectively, and the impurity is represented by $C$. The total number of quantum particles in leg $A$ and leg $B$ is conserved, and the total number of particles in species $C$ is conserved separately and equal to 1. In the supercell approach, the local Hilbert space is of size $2 \times 2 \times 2 = 8$ for the case of hard-core bosons and of $3 \times 3 \times 2 = 18$ for soft-core bosons if the maximum allowed occupancy per species $A$, $B$ is 2. We thus restrict ourselves to relatively large repulsions (of the order of $U_1 = U_2 = 10$ for soft-core bosons and $U_1 = U_2 = \infty$ for hard-core ones) in each leg for the bath so that the restriction of the Hilbert space is not a serious limitation. The interaction between the bath and the impurity can, however, take any value.

We consider a system for which the density in each leg is $\rho_0 = 1/3$, to avoid the possibility of entering to a Mott insulating state in the ladder in which the symmetric sector would be gapped as well. The longitudinal hopping of the leg 1, leg 2, and the impurity hopping are taken equal value, $t_b = t_{\text{imp}} = 1$. We fix the size of the system to $L = 101$ sites per leg.

In t-DMRG, the singular value decomposition of a matrix of the order of $(d\chi) \times (d\chi)$ is needed [33] for a sweep through a bond between two lattice sites, where $d$ is the local Hilbert space dimension and $\chi$ is bond dimension which encodes the amount of entanglement in the system. At each time step, $(L - 1)$ such operations are performed. As the local Hilbert space can become large for soft-core bosons, we are limited to moderate values of $\chi$ to maintain reasonable computational times. We further use bond dimensions $\chi = 300, 500, 400, 600$ for hard-core boson and $\chi = 400$ for soft-core boson. Further details are provided in Appendix B.

The ground state of the bath $|GS_b\rangle$ is computed by using DMRG. We then add an impurity in the center of leg 1, at time $t = 0$,

$$
|\psi(t = 0)\rangle = d_{\frac{L+1}{2}}^\dagger |GS_b\rangle.
\tag{33}
$$

We then evolve the state $|\psi(t = 0)\rangle$ as a function of time $(t)$ with the full Hamiltonian (1) by using t-DMRG and compute

$$
|\psi(t)\rangle = e^{-iHt} d_{\frac{L+1}{2}}^\dagger |GS_b\rangle.
\tag{34}
$$

We then take the overlap with the state

$$
d_{\frac{L+1}{2}-x}^\dagger |GS_b\rangle,
\tag{35}
$$

which yields the sought-after impurity Green's function in time and space, up to a phase factor of $e^{iE_{GS_b}t}$, where $E_{GS_b}$ is the ground-state energy of the bath. A Fourier transformation then yields the Green's function in time and momentum.
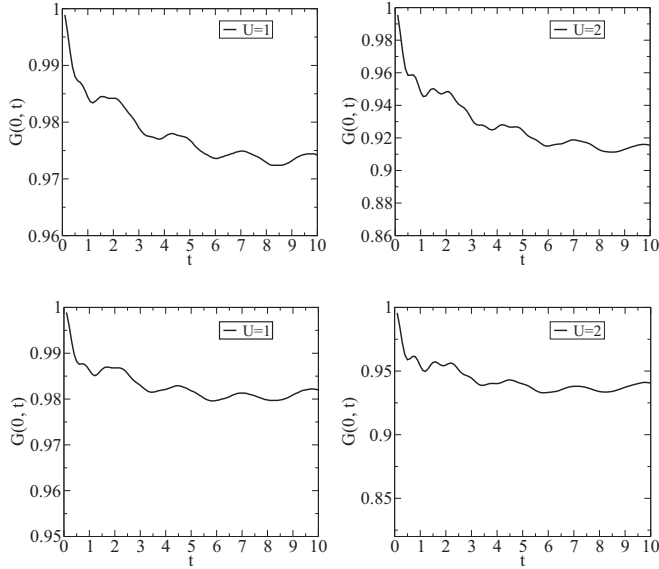
FIG. 3. Modulus of the Green's function of the impurity (see text) $|G(p = 0, t)|$ at zero momentum of the impurity. Parameters for the interchain hopping, impurity hopping, and impurity-bath interaction in the ladder are respectively $t_\perp = 1$, $t_{\mathrm{imp}} = 1$. Left (right) column corresponds to $U = 1$ ($U = 2$). The upper panel shows $|G(0, t)|$ of softcore bosons with $U_1 = U_2 = 10$ and the lower panel hardcore bosons for $\chi = 400$.

### B. Results at zero momentum

We examine first the Green's function of the impurity $G(p, t)$ for the case of zero momentum $p = 0$. For a single chain, this limit is known to lead to a power-law decay of the Green's function [8,12,15].

Examples of the decay of $|G(0, t)|$ are shown in Fig. 3, both for soft-core bosons and hard-core bosons. The numerical data shows a decay of the correlation function with time. Such a decay is expected from the general arguments of Sec. III. As discussed in Appendix B, the bond dimension controls the maximum time at which the decay of the correlation can be computed reliably with the t-DMRG procedure. In our case, the time of the order $t \sim 7$ for soft-core and $t \sim 7$ for hard-core bosons presents the limit for reliable data.

#### 1. Interaction dependence

To analyze the data we use the analytic estimates of Sec. III which suggest a power-law decay of the Green's function:

$$|G(p = 0, t)| \propto \left(\frac{1}{t}\right)^\alpha. \tag{36}$$

We fit the numerical data as detailed in Appendix B, which confirms the power-law decay of the correlations and allows extracting the exponent $\alpha$. This exponent is shown in Fig. 4 for the case of hard-core bosons.

The good agreement between the numerical exponent of Fig. 4 with the LCE formula in (25) confirms the analytic prediction of Sec. III that one can indeed view the ladder with a small impurity-bath interaction $U$ as a single TLL with an effective $K_s$ and $u_s$ but with an effective interaction $U/\sqrt{2}$. The simple decoupling of the Hamiltonian into the
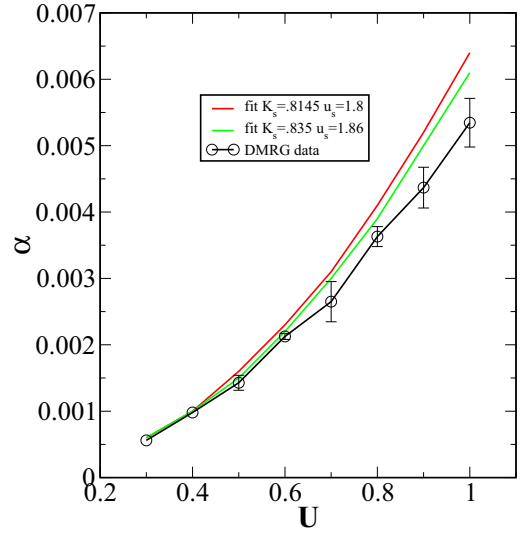


FIG. 4. Green's function exponent at $p = 0$ for hardcore bosons as function of small $U$ at $t_\perp = t_{\mathrm{imp}} = 1$. The black curve is the exponent extracted from correlation functions computed from t-DMRG results with $\chi = 600$. The green and red curves are the LCE exponent extracted from (25), $\alpha_{LCE} = \frac{K_s U^2}{4\pi^2 u_s^2}$, for the pair of values $(K_s = 0.835, u_s = 1.86)$, $(K_s = 0.8145, u_s = 1.8)$, respectively. These values correspond well to the TLL parameters for a ladder of hard-core bosons (see text).

symmetric and antisymmetric sector of (21) would naively suggest that $(K_s, u_s) = (K, v)$ of a single chain, but for large $U_1 = U_2$ interactions and sizable $t_\perp$, irrelevant operators can lead to a sizable renormalization of the parameters. So, in general, the parameters $(K_s, u_s)$ for the ladder are not identical to the ones of a single chain with the same interaction, also leading to a modification of the exponent. This is in particular the case for hard-core bosons, for which the single chain parameter is $K = 1$ [26], while for the ladder [32] one has $K_s < 1$ Our calculations yield $K_s = 0.8145$ and $u_s = 1.8$. Given the accuracy of determination of the TLL parameters this compares well with the values obtained in Ref. [32], which are $K_s = 0.835$ and $u_s = 1.86$ (cf. also Fig. 19 of [32]). We note that the single chain value of $K < 1$ would have meant that the backscattering on the impurity terms could become relevant. For the ladder case, however, because the antisymmetric sector is gapped, such terms remain irrelevant even for $K_s < 1$.

For larger values of the impurity-bath interaction $U$ one cannot rely on the LCE expression anymore. The numerically computed exponent is shown in Fig. 5. The quadratic growth of the exponent with the interaction of Fig. 4 is replaced by a more complex behavior and a saturation of the exponent at large $U$. For the single chain the interaction dependence of the exponent could be captured by an analytic expression [15]. In order to adapt this expression to the case of the ladder we use the modified interaction $U/\sqrt{2}$ suggested by the bosonization formula of Sec. III and the TLL parameters of the ladder which leads to

$$\alpha = \frac{2f}{\pi^2}\left(\arctan\left[\frac{2\sqrt{2f u_s^2}}{U\sqrt{K_s}}\right] - \frac{\pi}{2}\right)^2. \tag{37}$$
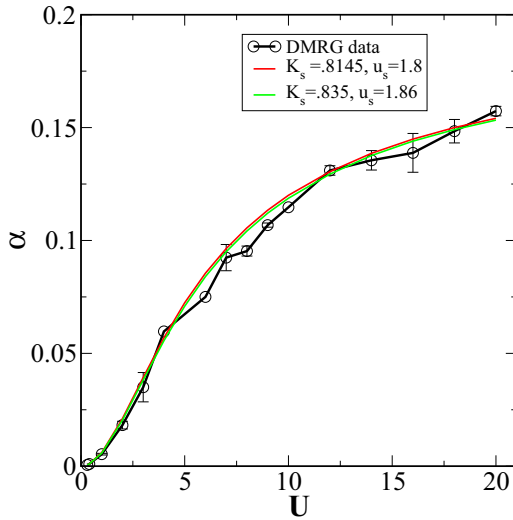
FIG. 5. Exponent $\alpha$ controlling the power-law decay of $|G(p = 0, t)|$ as a function of the interaction between the bath and the impurity $U$. The bath has $t_\perp = t_{\rm imp} = 1$ and is made of hard-core bosons at $1/3$ filling for each leg. The black circles are the numerical data. The red line is a fit to (37) (see text) with $f = 0.39$. The good agreement between the data and the formula (37) shows that, as for a single chain, this formula correctly describes the behavior of the impurity in the ladder for a wide range of interactions.

Here, $f = 2\alpha[U \to \infty]$, and we use the independently calculated exponent at $U = \infty$ (see next section) to obtain $f = 0.39$ for plotting the analytical curves in Fig. 5. We stress that the excellent agreement between DMRG data and analytical prediction Eq. (37) shown in Fig. 5 is thus without fitting parameters, unlike that in Ref. [15], which had been lacking an independent way of obtaining $f$ quantitatively.

### *2. Hard-core bath-impurity repulsion*

Let us now turn to the case for which the repulsion between the impurity and particles of the bath is very large $U \to \infty$. Various decays of the Green's function are shown in Fig. 6. As is clear from the numerical data, the power-law decay is still present in this limit and persists for all the measured values of $t_\perp$ in the ladder. A fit of the numerical data provides access to the exponent as a function of interchain hopping, as shown in Fig. 7.

We first note that the value of the exponent for $U = \infty$ at $t_\perp = 1$, $\alpha = 0.195$ is in good agreement with the one given by the formula (32) in which the interaction $U$ would be replaced by its phase shift as for the single chain [12] where $U \to U_\phi = v\pi$ in the formula $\frac{K_s U^2}{4\pi^2 u_s^2}$. Larger values of $t_\perp$ show a marked increase of the exponent as is evident from Fig. 4. This trend of the exponent with $t_\perp$ is surprising and is *a priori* not compatible with this extrapolation. In such a limit, the exponent would be proportional to $K_s$, which *decreases* when $t_\perp$ increases at variance with the numerical data. This shows that there is a dependence on $t_\perp$ of the exponent besides the one hidden in the $t_\perp$ dependence of the TLL parameters. How to compute this dependence analytically remains a challenge for the moment.
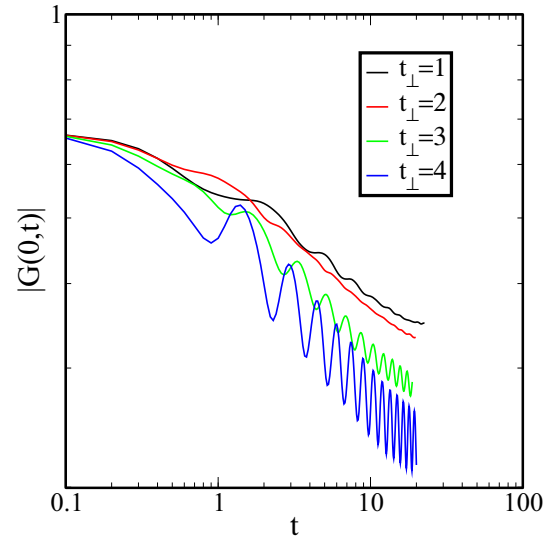


FIG. 6. Green's function of the impurity at zero momentum on a log-log scale for the ladder of hard-core bosons and for infinite repulsion between impurity and bath particles. $t_\perp = 1, 2, 3, 4$ and $t_b = t_{\rm imp} = 1$. The t-DMRG has been performed for $\chi = 600$. The power-law decay of the correlation is present for all measured values of $t_\perp$.

### C. Momentum dependence of the exponent

We now turn to the momentum dependence of the Green's function, which, as for the single chain, is much more difficult to obtain analytically.

We show in Fig. 8 the decay of the Green's function for various momenta $p$ of the impurity. The top panel, for small momentum of the impurity, shows a power-law decay of the Green's function, similar to the one for zero momentum, albeit with a renormalized exponent. However, above a momentum
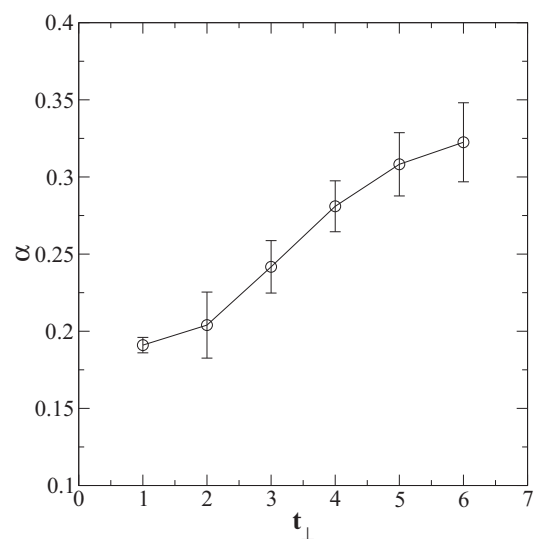


FIG. 7. Exponent of the Green's function of an impurity with a hard-core repulsion with a bath of hard-core bosons at filling $1/3$ as a function of $t_\perp$ at $t_{\rm imp} = 1$, $U \to \infty$, and $p = 0$. Circles are the numerical data for $\chi = 600$ and the line is a guide to the eyes.
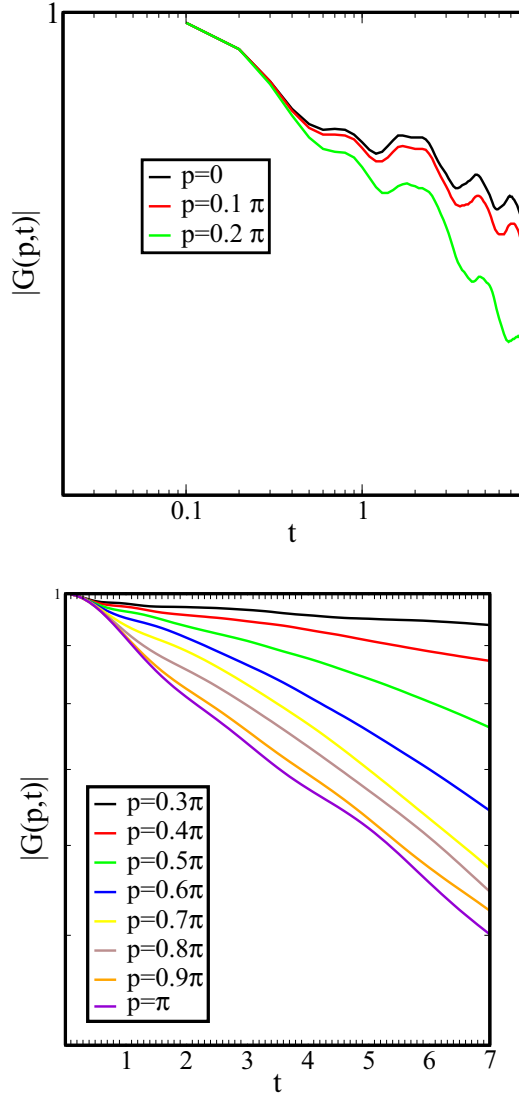
FIG. 8. Green's function of the impurity in a ladder of hard-core bosons, $t_{\rm imp} = 1$, and transverse hopping ($t_\perp = 1$), $U = 1$, for different momenta and $\chi = 600$. Upper panel: Green's function on log-log scale. The momenta are $p = 0, 0.1\pi, 0.2\pi$. On a log-log scale, the Green's functions show a linear behavior which reflects the power-law decay. Lower panel: Green's function on semilog plot. Momenta are $p = 0.3\pi, 0.4\pi, 0.5\pi, 0.6\pi, 0.7\pi, 0.8\pi, 0.9\pi, \pi$. On the semilog scale, the Green's function shows a linear behavior which reflects the exponential decay.

threshold around $0.3\pi$ the numerical data no longer exhibits a power-law decay and is fitted better with exponential decay, as shown in the lower panel of the figure. This is similar to the behavior observed for an impurity coupled to a single chain [15].

For small momentum, a momentum dependent exponent can be extracted by the fitting methods described in Appendix C. The results are shown in Fig. 9. The growth of the exponent with momentum can be expected since on general grounds one finds [8,15] that the exponent varies as

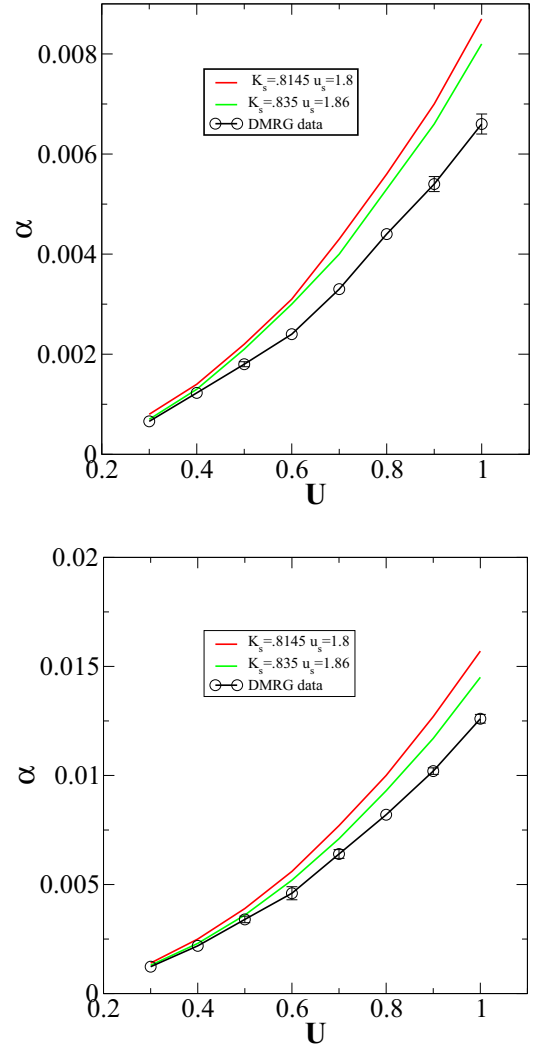$$\alpha(p) = \alpha(p = 0) + \beta p^2. \tag{38}$$



FIG. 9. Green's function exponent of the impurity in a ladder of hard-core bosons, as a function of $U$ for $p = 0.1\pi$ (upper panel), $0.2\pi$ (lower panel), $t_{\rm imp} = 1$, transverse hopping ($t_\perp = 1$), and $\chi = 600$. The black curves represent the DMRG data, and the green and red curves are fitted curves of the link cluster result with the TLL parameters mentioned in the inset.

The coefficient $\beta$ can be computed for small interactions (see Appendix A) and is given by

$$\beta = \frac{3K_s U^2}{\pi^2 u_s^2} \frac{t_{\rm imp}^2}{u_s^2}. \tag{39}$$

Comparison between the numerics and the LCE shows a very good agreement between the two for small interactions.

This good agreement with the numerical exponent and the LCE one suggests that as for the single chain we can use the LCE to estimate the critical momentum $p^*$ which separates the ID regime from the polaronic one. The crossover depends on the TLL characteristics of the bath, namely the velocity of sound in the ladder and the TLL parameter $K$. Using the values extracted from [32] we get
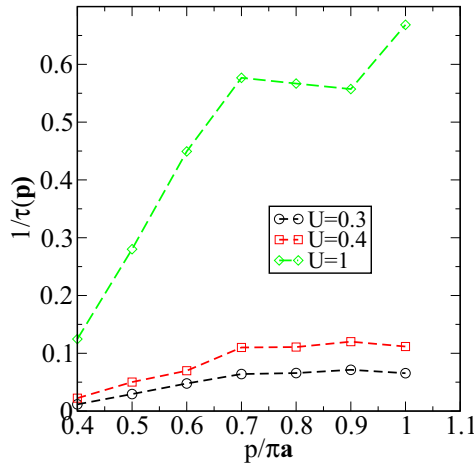
$$p^* = 0.3\pi, \tag{40}$$

FIG. 10. Inverse lifetime of the impurity as function of the momentum for a bath of hard-core bosons at one-third filling. The parameters are $t_{\text{imp}} = t_b = t_\perp = 1$, $U = 0.3, 0.4, 1$, $a = 1$ is lattice spacing.

which is in reasonably good agreement with the observed change of behavior in Fig. 8. Beyond the LCE we also see that the change of behavior is in good agreement with the criteria of intersection discussed in Fig. 2 when one uses properly the structure factor the ladder.

Beyond $p = p^*$ and for small $U$, the Green's function decays exponentially, the impurity behaves like a quasiparticle, and the Green's function of the impurity in terms of lifetime $\tau(p)$ is given by

$$|G(p, t)| = \exp[-t/\tau(p)]. \quad (41)$$

In Fig. 10, we plot the inverse of lifetime $1/\tau(p)$, defined in Eq. (41) of the QP as function of $p$ for different interactions $U = 0.3, 0.4, 1$. As can be expected $1/\tau(p)$ increases with increasing interaction. Let us now turn to the limit of infinite repulsion between the impurity and the bath. The numerical Green's functions are given in Fig. 11. In a similar way than for the small interaction limit, the numerical data shows a crossover from a power-law regime to another type of decay upon increasing the momentum. The transition occurs for after $p$ around $p^* = 0.9\pi$.

## V. DISCUSSION

Let us now discuss the various results for the ladder systems in comparison with the case for which the bath is a single chain. The motion of the impurity being still strictly one-dimensional all differences are directly related to the change of nature of the bath.

Let us first turn to the weak coupling between the bath and the impurity. The numerical results fully confirm that in such limit the field theory description (25) gives an excellent approximation of the exponent at zero momentum. The fact that only the symmetric mode is massless roughly leads to the replacement of the interaction between bath and impurity by $U/\sqrt{2}$. This would lead, if the TLL parameters were identical for the symmetric modes and a single chain, to a *reduction* of the exponent. This trend can be easily extended
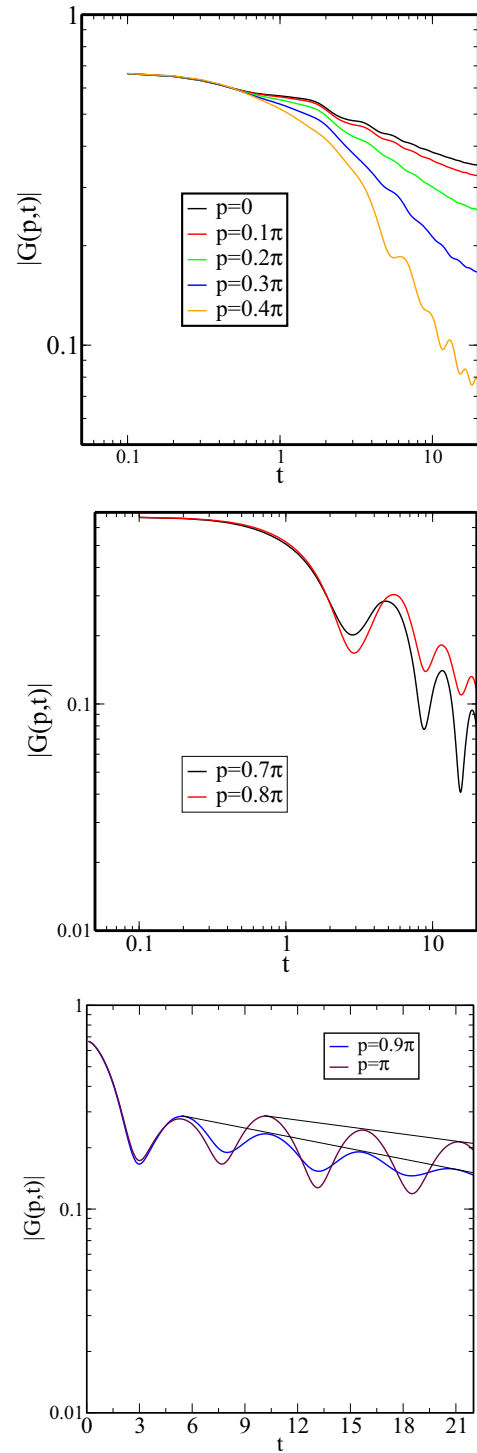


FIG. 11. Green's function of the impurity as a function of time for $p = 0, 0.1\pi, 0.2\pi, 0.3\pi, 0.4\pi, 0.7\pi, 0.8\pi, 0.9\pi, \pi$ for hard-core boson on log-log ($p = 0$–$0.8\pi$) scale and semilog scale ($p = 0.9\pi, \pi$), $t_\perp = 1.5$, $U = \infty$, $t_{\text{imp}} = 1$, for bond dimensions $\chi = 600$.

to a bath consisting of an $N$-leg bosonic ladder. In that case, all modes, except the global symmetric mode, are gapped, and the interaction with the impurity would become $U/\sqrt{N}$. Note that such a ladder with a large number of legs is very close to an anisotropic two-dimensional superfluid [34].

We, however, see that some of the peculiarities of the ladder, which would likely disappear when increasing the number of legs, manifest themselves in the exponent in addition to the effect as mentioned above. The ladder itself is more affected by the interactions *within* the bath than a single chain. This is readily seen by the fact that a ladder of hard-core bosons at a filling of one boson per rung would be an insulator, while a single chain remains a superfluid at half filling. As a consequence the TLL parameter $K$ can reach values below one [32] corresponding to "enhanced" repulsion compared to the case of a single chain. This effect also contributes to the decay and to a further reduction of the exponent compared to the effect on $U$ itself.

On the other hand, increasing $t_\perp$ leads to an opposite trend, particularly visible in the limit of large $t_\perp$ (see Fig. 7), in which a marked *increase* of the exponent can be seen. Naively one could consider that increasing $t_\perp$ brings back the system to a single mode for the rung and thus pushes the system back to a more one-dimensional behavior. However, the impurity couples still to both modes making the calculation of the exponent delicate. How such effects would be modified upon increasing the number of legs is, of course, an interesting and open question.

As can be seen from Fig. 5 the general expression that was introduced in [15] provides a good description of the decay exponent at zero momentum for the ladder as well. Note that in the present case we have a full numerical evaluation of the infinite repulsion case between impurity and the bath, making it an essentially parameter-free formula and allowing one to check that the large impurity-bath repulsion limit is indeed correctly reproduced by this formula. This confirms that for a system in which the impurity couples to a single massless mode the generalization of the free fermion solution (37) captures the essential physics, and we would expect it to hold to the case of $N$ chains as well. As for the single chain, the finite momentum case remains more difficult to interpret. We recover for the ladder the same two regimes that were observed in the single chain, namely a regime dominated by infrared divergences (ID) for which we have the power-law decay of the correlations and a different regime, which seems, within the accuracy of the numerical solution also, to correspond to a faster decay of the correlations, and thus to a more conventional polaronic regime. As for the single chain, the separation between these two regimes seems to be reasonably well given by the possibility to excite real particle-hole excitations in the bath, as shown by Fig. 2.

Finally, let us note that the analysis of the present paper is made for a repulsive interaction between the impurity and the bath. The attractive case is more complex because of the possibility of forming a bound state between the impurity and a particle of the bath [35]. Note that such a bound state formation has also been reported in the two-dimensional case [36–38]. How such a bound state would affect the results or not compared to the repulsive case is an interesting question which would deserve a separate analysis going beyond the scope of the present paper. Note that a simple extrapolation of the LCE result for weak coupling would show no dependence on the sign of the interactions.

## VI. CONCLUSION AND PERSPECTIVES

We have studied the effect of a quantum bath made of a bosonic ladder on an impurity confined to move in one dimension. We have computed, both analytically and by using the time-dependent density-matrix renormalization group, the Green's function of the impurity as a function of the interaction between the impurity and the bath and the interactions in the bath itself.

We find that, as for a single chain bath, the presence of the bath affects the mobility of the impurity drastically, in a way quite different than a simple renormalization of the mass of the impurity via a polaronic effect. One measure of such effects is given by the Green's function of the impurity corresponding to the creation of an impurity with a given momentum $p$ at time zero and its destruction at time $t$. We compute this Green's function both analytically using a bosonization representation of the bath, linked cluster expansion and numerically with a time-dependent density-matrix renormalization-group technique.

We find that for small momentum the Green's function decays as a power law. For weak interaction between the impurity and the bath, the exponent is smaller than for a single chain, due to the gap appearing in the antisymmetric mode of the ladder. This trend would increase with the number of legs of the ladder, and reflect the trend to the more two-dimensional behavior. On the other hand, some aspects of the ladder are manifest in the fact that for large tunneling in the ladder one finds an increase of the exponent.

We also studied the dependence of the Green's function on the momentum of the impurity and found, in a similar way, that for the single chain there is a regime other than the power-law decay that appears, in which one has an exponential decay. The transition between these two regimes is well connected with the possibility to excite real rather than virtual particle-hole excitations in the bath.

Our analysis is a first step towards studying the evolution from the 1D behavior, essentially dominated by the Anderson orthogonality catastrophe provoked by the motion of the impurity, and which in 1D is not cured by the motion itself, and the higher-dimensional behavior, in which more conventional polaronic behavior is expected. Several additional directions could prove interesting extensions. If the interaction in the bath becomes sufficiently strong and sufficiently long range, backscattering on the bath becomes as relevant as the forward scattering considered in the present study. It would be interesting to know the effect on the impurity in ladders. Another extension could be to let the impurity also delocalize on the various chains so that the motion of the impurity itself tends to a two-dimensional one.

Cold atomic systems could provide a good realization of the systems described in the present paper. On one hand, bosonic ladders have been realized [39] and more generally systems made of many bosonic tubes are routinely realizable either in bulk [40] or in boson microscopes. Atom chips systems provide also an excellent realization of a ladder system [41]. Systems with bath and impurities have already been realized for single chains [22–25] either by using two species (such as K and Rb) or internal degrees of freedom.

Combination of these two aspects should be reachable in the very near future.

### APPENDIX A: LINKED CLUSTER EXPANSION

We have shown in the main text that for small interaction between impurity and ladder compared to the gap in the antisymmetric sector, the impurity effectively couples only to the forward scattering part of the symmetric sector. We give in this Appendix the LCE calculation of the Green's function of the impurity for a weak interaction $U$. We consider the symmetric part of (21) as the bath Hamiltonian and represent it in terms of the usual bosonic operators [26].

In the second quantized notation (23) is described by

$$
\begin{aligned}
H &= H_s + H_{\text{imp}} + H_{\text{coup}}, \\
H_s &= \sum_q u_s |q| b_{sq}^\dagger b_{sq}, \\
H_{\text{coup}} &= \sum_{q,k} V(q) d_{k+q}^\dagger d_k (b_{sq} + b_{s-q}^\dagger), \\
H_{\text{imp}} &= \sum_q \epsilon(q) d_q^\dagger d_q,
\end{aligned} \tag{A1}
$$

where $b^\dagger$ and $d^\dagger$ are the creation operators for the bath and the impurity, respectively, $H_{\text{imp}}$ is the tight-binding Hamiltonian of the impurity, and $H_{\text{coup}}$ is the interaction between impurity and bath:

$$
V(q) = \frac{U}{\sqrt{2}} \sqrt{\frac{K_s |q|}{2\pi L}} \exp\left(-\frac{|q|}{2q_c}\right), \tag{A2}
$$

where $q_c$ is an ultraviolet cutoff of the order of the inverse lattice spacing.

The Green's function of the impurity is defined as

$$
G(p,t) = -i \langle d_p(t) d_p^\dagger(0) \rangle. \tag{A3}
$$

By using LCE, Eq. (A3) can be written as

$$
G(p,t) = -i \, e^{-i\epsilon_p t} e^{F_2(p,t)}, \tag{A4}
$$

where $F_2(p,t)$ is defined as

$$
F_2(p,t) = e^{i\epsilon_p t} W_2(p,t). \tag{A5}
$$

$W_2(p,t)$ is given by

$$
\begin{aligned}
W_2(p,t) = &-\frac{1}{2} \int_0^t dt_1 \int_0^t dt_2 \\
&\times \langle T_\tau d_p(t) H_{\text{coup}}(t_1) H_{\text{coup}}(t_2) d_p^\dagger(0) \rangle.
\end{aligned} \tag{A6}
$$

By employing Wick's theorem $W_2(p,t)$ is given by

$$
\begin{aligned}
W_2(p,t) = &-\sum_q V(q)^2 \int_0^t dt_1 \int_0^t dt_2 Y(t_1) e^{-i\epsilon(p)t_1} \\
&\times Y(t_2 - t_1) e^{-i\epsilon(p+q)(t_2-t_1)} Y(t-t_2) \\
&\times e^{-i\epsilon(p)(t-t_2)} Y(t_2-t_1) e^{-i[u_s|q|(t_2-t_1)]},
\end{aligned} \tag{A7}
$$

where $Y(t)$ is a step function, which is zero for $t < 0$ and one for $t > 0$. $Y(t)$ changes the limit of integration of $t_2$ and $t_1$, and $F_2(p,t)$ is modified as

$$
\begin{aligned}
F_2(p,t) = &-\sum_q V(q)^2 \int_0^t dt_2 \int_0^{t_2} dt_1 e^{-i\epsilon(p)t_1} \\
&\times e^{-i\epsilon(p+q)(t_2-t_1)} \\
&\times e^{-i\epsilon(p)(t-t_2)} e^{-i[u_s|q|(t_2-t_1)]},
\end{aligned} \tag{A8}
$$

$$
\begin{aligned}
F_2(p,t) = &-\sum_q \int du \, V(q)^2 \int_0^t dt_2 \int_0^{t_2} dt_1 \\
&\times e^{-it_1 u} e^{it_2 u} \\
&\times \delta(u - [\epsilon(p) - \epsilon(p+q) - u_s|q|]).
\end{aligned} \tag{A9}
$$

After performing an integration over $t_1$ and $t_2$, $F_2(p,t)$ is given by

$$
\begin{aligned}
F_2(p,t) = &-\sum_q \int du \, V(q)^2 \\
&\times \frac{1 + iut - e^{itu}}{u^2} \\
&\times \delta(u - [\epsilon(p) - \epsilon(p+q) - u_s|q|]),
\end{aligned} \tag{A10}
$$

which can be rewritten as

$$
F_2(p,t) = -\int du \frac{1 + iut - e^{itu}}{u^2} R(u). \tag{A11}
$$

For small momentum $\epsilon(p) \simeq t_{\text{imp}} p^2$,

$$
R(u) = \sum_q V(q)^2 \delta(u - [\epsilon(p) - \epsilon(p+q) - u_s|q|]). \tag{A12}
$$

We evaluate $R(u)$ as

$$
R(u) = \frac{1}{2\pi} \int dq \, V(q)^2 \delta(u - [\epsilon(p) - \epsilon(p+q) - u_s|q|]). \tag{A13}
$$

$q$'s roots inside the delta function are given by

$$
q_{\pm}^{>} = -\left(p + \frac{u_s}{2t_{\text{imp}}}\right) \pm \sqrt{\left(p + \frac{u_s}{2J}\right)^2 - \frac{u}{t_{\text{imp}}}} \tag{A14}
$$

and

$$
q_{\pm}^{<} = -\left(p - \frac{u_s}{2t_{\text{imp}}}\right) \pm \sqrt{\left(p - \frac{u_s}{2t_{\text{imp}}}\right)^2 - \frac{u}{t_{\text{imp}}}}. \tag{A15}
$$

$q^{>}$ corresponds to $q > 0$ and $q^{<}$ corresponds to $q < 0$. For $(p - \frac{u_s}{2t_{\text{imp}}}) < 0 \wedge u > 0$, $R(u) = 0$, while for

$(p - \frac{u_s}{2t_{\text{imp}}}) > 0 \wedge u > 0$ one has

$$R(u) = \frac{1}{2t_{\text{imp}}} \left[ \left( \frac{p - u_s/(2t_{\text{imp}})}{\sqrt{[p - u_s/(2t_{\text{imp}})]^2 - u/t_{\text{imp}}}} - 1 \right) \right.$$

$$\times e^{-|q_+^{\leq}|/(2q_c)} + \left( \frac{p - u_s/(2t_{\text{imp}})}{\sqrt{[p - u_s/(2t_{\text{imp}})]^2 - u/t_{\text{imp}}}} + 1 \right)$$

$$\left. \times e^{-|q_-^{\leq}|/(2q_c)} \right]. \tag{A16}$$

For $u < 0$,

$$R(u) = \frac{1}{2t_{\text{imp}}} \left[ \left( 1 - \frac{p + u_s/(2t_{\text{imp}})}{\sqrt{[p + u_s/(2t_{\text{imp}})]^2 - u/t_{\text{imp}}}} \right) \right.$$

$$\times e^{-|q_+^{>}|/(2q_c)}$$

$$\left. + \left( \frac{p - u_s/(2t_{\text{imp}})}{\sqrt{[p - u_s/(2t_{\text{imp}})]^2 - u/J}} + 1 \right) e^{-|q_-^{\leq}|/(2q_c)} \right]. \tag{A17}$$

If $(p - \frac{u_s}{2t_{\text{imp}}}) < 0, \wedge u < 0$

$$R(u) \simeq u, \tag{A18}$$

$$\text{Re}[F_2(p, t)] \simeq -\ln(|t|). \tag{A19}$$

For small $|(p - \frac{u_s}{2t_{\text{imp}}})|$,

$$\text{Re}[F_2(p, t)] \simeq -\frac{K_s U^2}{4\pi^2 u_s^2} \left( 1 + \frac{12 t_{\text{imp}}^2 p^2}{u_s^2} \right) \ln(|t|), \tag{A20}$$

leading to the Green's function decay

$$|G(p, t)| = e^{-\frac{K_s U^2}{4\pi^2 u_s^2} \left( 1 + \frac{12 t_{\text{imp}}^2 p^2}{u_s^2} \right) \ln(|t|)}. \tag{A21}$$

## APPENDIX B: DMRG PROCEDURE

In Fig. 12, we show the Green's function of the impurity for $\chi = 300, 400, 500, 600$ at zero momentum. We find that the Green's function upturns after a certain time. This is because entanglement entropy scale linearly with time, so one needs exponentially large $\chi$ to get a good result. This is confirmed by studying the upticks behavior with increased $\chi$, which as a result is pushed out further and further in time, as shown in Fig. 12.

## APPENDIX C: EXTRACTING EXPONENT AND ERROR BAR FROM NUMERICAL DATA

The absolute value of Green's function of the impurity decays monotonically as a function of time but with superimposed oscillations. To extract the exponents, we first select all the data (up to a maximum time) where the Green's function
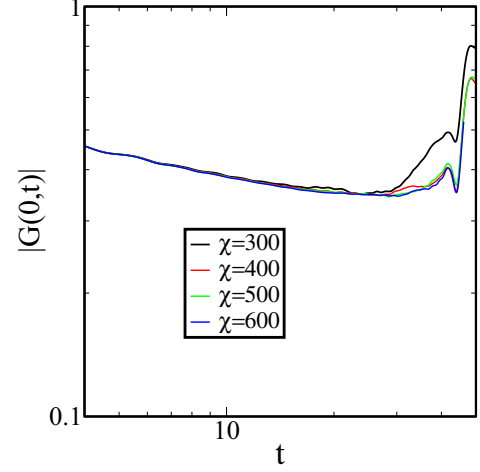


FIG. 12. Green's function as a function of time at $p = 0$ for hardcore boson, $t_{\perp} = 1.5$, $U = \infty$, $t_b = 1$, $t_{\text{imp}} = 1$ for bond dimensions $\chi = 300, 400, 500, 600$. With increasing $\chi$ the upturn of the Green's function is pushed out further in turn and is thus revealed as an artifact resulting from the exponential increase in entanglement with time.

displays local maxima. We compute the slope between two neighboring data and take the average of all the slopes to obtain the exponent.
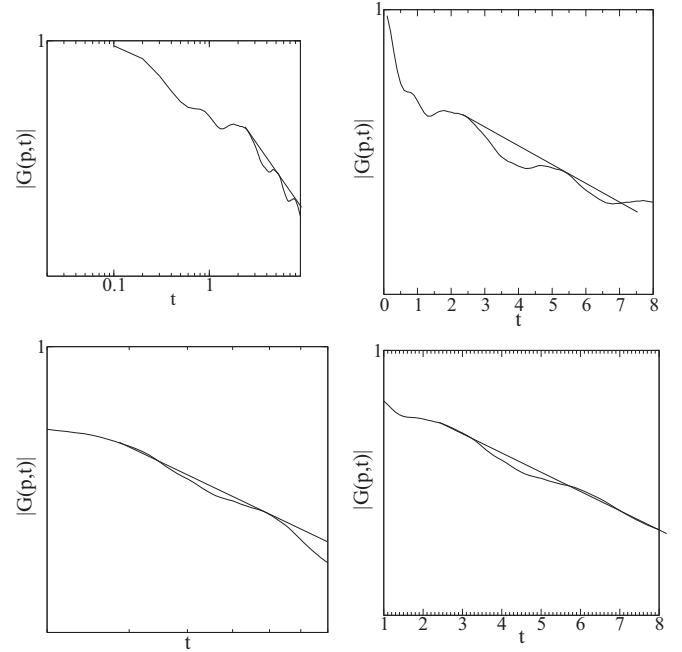


FIG. 13. Green's function of the impurity as function of time for hard-core bosons at $t_{\text{imp}} = t_b = 1$, $t_{\perp} = 1$, and $U = 1$. The upper panel represents the Green's function at $p = 0.2\pi$ and the lower panel the Green's function at $p = 0.3\pi$ on log-log scale (left) and semilog scale (right). At $p = 0.2\pi$, the Green's function is linear on a log-log scale but deviates on a semilog scale from linear behavior. On the other hand, at $p = 0.3\pi$, the Green's function is linear on a semilog scale but deviates on a log-log scale from linear behavior. This allows us to fix $p^* \sim 0.3\pi$ as the critical momentum at which the decay for the impurity goes from power law to exponential.

We take $\log_{10}|G(0, t_l)|$'s to denote the maxima of $\log_{10}|G(0, t)|$, at time $t_l$, where $l = 1, 2, \ldots, n$. Then the slope between time $t_l$ and $t_{l+1}$ is given by $\beta_l = \frac{\log_{10}[|G(0,t_l)|] - \log_{10}[|G(0,t_{l+1})|]}{\log_{10}(t_{l+1}) - \log_{10}(t_l)}$ and the exponent $\alpha = \frac{\beta_1 + \beta_2 + \cdots \beta_{n-1}}{n-1}$. The error bar is given by $\frac{|\alpha - \beta_1| + |\alpha - \beta_2| + \cdots + |\alpha - \beta_{n-1}|}{n-1}$.

To distinguish between a power-law decay and an exponential one, and determine the critical momentum $p^*$ at which such a change occurs, we show in Fig. 13 the Green's function of impurity at $U = 1$, $p = 0.2\pi$ on both log-log scale and semilog scale.

The comparison both on a log-log scale and a semilog one of these two behaviors allows us to determine $p^* \sim 0.3\pi$ at which the change of behavior from power law to exponential occurs. At $p = 0.2\pi$, the Green's function decays but has oscillations. To extract the exponent we select all the points where the Green's function is maximum and use the above procedure to compute the error bars and exponent.

[1] R. P. Feynman, Phys. Rev. **97**, 660 (1955).

[2] R. P. Feynman, *Statistical Mechanics* (Benjamin, Reading, MA, 1972).

[3] L. D. Landau, J. Exp. Theor. Phys. **3**, 920 (1957).

[4] P. Nozieres, *Theory of Interacting Fermi Systems* (Benjamin, New York, 1961).

[5] A. O. Caldeira and A. J. Leggett, Ann. Phys. (NY) **149**, 374 (1983).

[6] A. J. Leggett, S. Chakravarty, A. T. Dorsey, M. P. A. Fisher, A. Garg, and W. Zwerger, Rev. Mod. Phys. **59**, 1 (1987).

[7] F. Grusdt and E. Demler, New theoretical approaches to Bose polarons, notes of the International School of Physics Enrico Fermi, Varenna, Italy (unpublished), arXiv:1510.04934.

[8] M. B. Zvonarev, V. V. Cheianov, and T. Giamarchi, Phys. Rev. Lett. **99**, 240404 (2007).

[9] A. Kamenev and L. I. Glazman, Phys. Rev. A **80**, 011603(R) (2009).

[10] K. A. Matveev and A. Furusaki, Phys. Rev. Lett. **101**, 170403 (2008).

[11] M. Schecter, A. Kamenev, D. M. Gangardt, and A. Lamacraft, Phys. Rev. Lett. **108**, 207001 (2012).

[12] A. Lamacraft, Phys. Rev. B **79**, 241105(R) (2009).

[13] M. B. Zvonarev, V. V. Cheianov, and T. Giamarchi, Phys. Rev. Lett. **103**, 110401 (2009).

[14] M. B. Zvonarev, V. V. Cheianov, and T. Giamarchi, Phys. Rev. B **80**, 201102(R) (2009).

[15] A. Kantian, U. Schollwöck, and T. Giamarchi, Phys. Rev. Lett. **113**, 070601 (2014).

[16] F. Massel, A. Kantian, A. J. Daley, T. Giamarchi, and P. Törmä, New J. Phys. **15**, 045018 (2013).

[17] B. Horovitz, T. Giamarchi, and P. Le Doussal, Phys. Rev. Lett. **111**, 115302 (2013).

[18] C. J. M. Mathy, M. B. Zvonarev, and E. Demler, Nat. Phys. **8**, 881 (2012).

[19] M. Knap, C. J. M. Mathy, M. Ganahl, M. B. Zvonarev, and E. Demler, Phys. Rev. Lett. **112**, 015302 (2014).

[20] S. I. Mistakidis, G. C. Katsimiga, G. M. Koutentakis, T. Busch, and P. Schmelcher, Phys. Rev. Lett. **122**, 183001 (2019).

[21] B. Horovitz, T. Giamarchi, and P. Le Doussal, Phys. Rev. Lett. **121**, 166803 (2018).

[22] S. Palzer, C. Zipkes, C. Sias, and M. Köhl, Phys. Rev. Lett. **103**, 150601 (2009).

[23] J. Catani, G. Lamporesi, D. Naik, M. Gring, M. Inguscio, F. Minardi, A. Kantian, and T. Giamarchi, Phys. Rev. A **85**, 023623 (2012).

[24] T. Fukuhara, A. Kantian, M. Endres, M. Cheneau, P. Schauß, S. Hild, D. Bellem, U. Schollwöck, T. Giamarchi, C. Gross *et al.*, Nat. Phys. **9**, 235 (2013).

[25] F. Meinert, M. Knap, E. Kirilov, K. Jag-Lauber, M. B. Zvonarev, E. Demler, and H.-C. Nägerl, Science **356**, 945 (2017).

[26] T. Giamarchi, *Quantum Physics in One Dimension*, The International Series of Monographs on Physics (Clarendon Press, Oxford, 2004).

[27] S. R. White, Phys. Rev. Lett. **69**, 2863 (1992).

[28] U. Schollwöck, Rev. Mod. Phys. **77**, 259 (2005).

[29] N. A. Kamar, A. Kantian, and T. Giamarchi (unpublished).

[30] M. A. Cazalilla, R. Citro, T. Giamarchi, E. Orignac, and M. Rigol, Rev. Mod. Phys. **83**, 1405 (2011).

[31] E. H. Lieb and W. Liniger, Phys. Rev. **130**, 1605 (1963).

[32] F. Crépin, N. Laflorencie, G. Roux, and P. Simon, Phys. Rev. B **84**, 054517 (2011).

[33] U. Schollwöck, Ann. Phys. (NY) **326**, 96 (2011).

[34] M. A. Cazalilla, A. F. Ho, and T. Giamarchi, New J. Phys. **8**, 158 (2006).

[35] J. McGuire, J. Math. Phys. **7**, 123 (1966).

[36] M. Koschorreck, D. Pertot, E. Vogt, B. Fröhlich, M. Feld, and M. Köhl, Nature (London) **485**, 619 (2012).

[37] R. Schmidt, T. Enss, V. Pietilä, and E. Demler, Phys. Rev. A **85**, 021602(R) (2012).

[38] S. Zöllner, G. M. Bruun, and C. J. Pethick, Phys. Rev. A **83**, 021603(R) (2011).

[39] M. Atala, M. Aidelsburger, M. Lohse, J. T. Barreiro, B. Paredes, and I. Bloch, Nat. Phys. **10**, 588 (2014).

[40] T. Stöferle, H. Moritz, C. Schori, M. Köhl, and T. Esslinger, Phys. Rev. Lett. **92**, 130403 (2004).

[41] S. Hofferberth, I. Lesanovsky, T. Schumm, A. Imambekov, V. Gritsev, E. Demler, and J. Schmiedmayer, Nat. Phys. **4**, 489 (2008).

[42] https://people.smp.uq.edu.au/IanMcCulloch/mptoolkit/.